Received: 23 October 2020 | Revised: 18 May 2021 | Accepted: 31 May 2021

DOI: 10.1111/ddi.13367

RESEARCH ARTICLE

Diversity and Distributions WILEY

The role of dispersal limitation and reforestation in shaping the distributional shift of a forest herb under climate change

Frederik Van Daele | Olivier Honnay | Hanne De Kort

Plant Conservation and Population Biology, Department of Biology, KU Leuven, Leuven, Belgium

Correspondence
Frederik Van Daele, Plant Conservation and Population Biology, Department of Biology, KU Leuven, Kasteelpark Arenberg 31, 3001, Leuven, Belgium.
Email: frederik.vandaele@kuleuven.be

Funding information
Fonds Wetenschappelijk Onderzoek, Grant/Award Number: G091419N

Editor: Luca Santini

Abstract

Aim: Forest herbs might be unable to track shifts in habitat suitability due to rapid climate change and habitat fragmentation. In this study, we quantified the role of dispersal limitation and the potential mitigating effect of large-scale reforestation on the redistribution of the herbaceous forest plant species *Primula elatior* under climate change.

Location: Europe.

Methods: High resolution (100 m) landscape-scale and macro-climatic variables were combined to predict range-wide habitat suitability using Maxent. Dispersal limitation was modelled, based on isolation-by-resistance (IBR) principles through integration of circuit theory and genomic data, to assess patch accessibility and metapopulation stability under climate change. Large-scale reforestation was evaluated as a potential mitigating strategy by incorporating a land use change scenario into the distribution and dispersal models.

Results: Landscape-scale variables contributed significantly to the distribution of *P. elatior* (78.33%) and to the accuracy of our model (AUC = 0.81). Isolation-by-resistance (R^2_{cond} = .92) was driven by land use (45.5%), distance from rivers (36.4%) and elevation (18.2%). It was estimated that 46.4 ± 13.9% (mean ± *SD* of climate change scenarios) of the total distribution area would be lost due to climate change by 2050 and an additional 15.6 ± 1.7% (mean ± *SD*) of the distribution would not be accessible through migration. The median latitude of the patch distribution shifted 183.2 ± 34.8 km (mean ± *SD*) northwards and 58.1 ± 9.3 km (mean ± *SD*) to more maritime regions. The patch accessibility was low in these regions and the metapopulation stability decreased considerably in the south of the distribution. Reforestation mitigated 54.1 ± 18.2% (mean ± *SD*) of the accessible distribution area loss and 49.5 ± 4.2% (mean ± *SD*) of the decrease in metapopulation stability.

Main conclusion: To alleviate the loss of the accessible distribution area of *P. elatior* under climate change, it will be required to integrate climate mitigation strategies (RCP 2.6), range-wide afforestation, restoration of ecological connectivity and focused assisted migration to newly available habitat.

KEYWORDS
climate change, dispersal limitation, distribution shift, forest ecology, habitat fragmentation, plant ecology, plant migration, reforestation, species distribution modelling

1 | INTRODUCTION

Global temperature and precipitation patterns are rapidly changing and are expected to severely affect the distribution of many plant species (Thuiller et al., 2005). Land temperatures in different European regions are projected to increase further by 1.4 and 4.2°C under Representative Concentration Pathway (RCP) 4.5 scenario and by 2.7 to 6.2°C under the RCP 8.5 scenario (by 2071–2100, compared to 1971–2000) (European Environment Agency, 2020). Furthermore, climate models have shown a high probability of increasing intensity and duration of droughts by the end of the century (Cook et al., 2020). As a consequence, a general latitudinal range shift of plants is expected from south to north (Lenoir & Svenning, 2015).

Europe is among the most forest-rich regions in the world, with forest covering 34% (EU27) of its total land area. However, forests and their understorey vegetation are heavily impacted by anthropogenic influences, increasing their sensitivity to global changes (European Commission, 2011). The understorey in temperate forests is often species-rich, provides food and shelter for many other organisms and mediates ecosystem processes such as tree regeneration, nutrient cycling and evapotranspiration (Landuyt et al., 2019). Forest herbs require very specific habitat conditions and are often highly dispersal limited. Many forest herbs will therefore be unable to track climate-induced shifts in their habitat distribution (Honnay et al., 2002). In-depth modelling of how global change drivers affect specific forest herbs on a local, regional and continental scale have the potential to guide mitigation strategies to safeguard the diversity and functioning of temperate forests. However, integrated modelling approaches that predict changes in the habitat distribution of forest herbs under global change, and at the same time assess dispersal routes are challenging and require improved predictive capacity.

Species distribution models (SDMs) have provided valuable insights into range shifts of certain plant species under climate change scenarios (Guisan & Thuiller, 2005). Yet their accuracy can be limited because input data often do not cover the entire current extent of a species´ range and because predictions have too coarse resolutions. Furthermore, inferences in terms of local extinction and colonization are generally based on range shifts alone (Chave, 2013; Fordham et al., 2012; Guisan et al., 2017). To reliably use SDMs for biological conservation, ecological restoration and impact mitigation, it is necessary to use a predictor resolution and response accuracy which accurately reflect the species' ecological niche breadth (Connor et al., 2018), ideally covering its whole range (Lembrechts et al., 2018; Thuiller et al., 2015). This is especially true for habitat specialists such as herbaceous forest plant species, where the potential for establishment is determined by a complex interplay between biotic and abiotic interactions. Integrating landscape-scale variables that partly capture topoclimatic processes, such as fine-scale topography (Lassueur et al., 2006), land use classes (Sirami et al., 2017) and the presence of riparian zones (Moore et al., 2005), in SDMs may therefore considerably increase their accuracy (Clerici et al., 2013).

Apart from their specific habitat requirements, many forest herb species are also known to be strongly limited in their dispersal, hampering the colonization of new suitable habitat in areas where habitat fragmentation has surpassed a critical level (Ehrlén & Eriksson, 2000). To accurately assess whether habitat fragmentation impedes future range expansion, it is essential to assess the dispersal potential between currently occupied habitat patches and future suitable habitats (Bateman et al., 2013; Franklin, 2010). Recent advances in dispersal modelling allow for assessments of species-specific dispersal modes through genetic optimization of landscape connectivity (Peterman et al., 2019). Optimization methods rely on the expected relationship between landscape connectivity and genetic distance for selecting the most likely dispersal scenario. Whereas these optimization methods have successfully been applied to animal populations (Littlefield et al., 2017; Maiorano et al., 2019), they have rarely been used for habitat connectivity analysis in plants (Dickson et al., 2019). This is remarkable, because the importance of seed dispersal limitation in mediating range shifts is well known for specialist plant species (Ehrlén & Eriksson, 2000; Honnay et al., 2002; Skov & Svenning, 2004). Furthermore, accurate dispersal modelling of plant species is important in order to guide mitigation strategies such as assisted migration (Lunt et al., 2013) and connectivity restoration (Krosby et al., 2010) in the coming decades.

Changes in forest cover and composition will affect understorey habitat availability and may have a large impact on the dispersal and colonization potential of forest herbs undergoing climate change (Canadell & Raupach, 2008; Millar et al., 2007). Furthermore, future changes in forest cover and composition will directly affect habitat availability for understorey species (Nieto-Lugilde et al., 2015). Reforestation policy targets, as set by the European Commission, and natural regeneration on abandoned farmland are therefore expected to strongly affect the extent of species distribution shifts induced by climate change (European Commission, 2019; Guo et al., 2018). Although some studies have examined climate change effects on afforestation success (Duque-Lazo et al., 2018) and tree species distributions (Buras & Menzel, 2019), we are unaware of any studies that have integrated afforestation efforts in modelling the distribution of forest understory species under climate change scenarios.

Primula elatior was used as a study case because it is widespread and highly representative for other forest herbs from alluvial deciduous forests. Due to its specific habitat requirements, intolerance to desiccation, absence of seed dispersal mechanisms and self-incompatibility, it may be specifically sensitive to climate change and habitat fragmentation (Honnay et al., 2002; Taylor & Woodell, 2008). Here, we aimed to assess how climate change and afforestation/reforestation efforts would affect the amount of accessible habitat for

the forest herb *P. elatior*. To this end, we defined four research objectives (RO) which structure this study. First (RO I), we developed a habitat suitability model for *P. elatior* by integrating landscape-scale and macro-climatic variables, and projected its distribution under climate change by 2050. Second (RO II), we quantified the proportion of suitable habitat that is accessible through dispersal and long term migration, using circuit theory and genetic data. Third (RO III), we analysed shifts in the distribution of suitable habitat and assessed their implications for habitat accessibility and metapopulation stability under climate change by 2050. Finally (RO IV), we quantified the mitigation effect of envisioned continental large-scale reforestation on the future distribution of *P. elatior*.

2 | METHODS

2.1 | Study system

Primula elatior subsp. *elatior* (in the Primulaceae family) is a European riparian forest species, with the native distribution spanning from the north of Denmark and southern Sweden to the Pyrenees. In western France, the species is rare, and in Great Britain, the species is native in a few locations only. In the east, populations occur in the Baltic States, Poland and the north-eastern Carpathians in Ukraine and Romania (Taylor & Woodell, 2008). Successful introductions of *P. elatior* have occurred in Norway, which could suggest that the current range is restricted by dispersal limitation and not by the cold edge of its thermal niche (collected samples; Alm & Often, 2009).

Primula elatior typically occurs in sub-Atlantic and medio-European oak or oak-hornbeam forests of the alliance *Carpinion betuli* and to a lesser extent in alluvial forests with European alder and ash of the alliance *Alno-Padion* (Hennekens et al., 2010; Leuschner & Ellenberg, 2017). The species is known to have limited colonization capacity of newly established forests (Jacquemyn et al., 2002). Seeds fall from elevated stems and dispersal is generally driven by either gravity (barochory) or wind (rolling anemochory; Endels et al., 2004). Occasionally, however, long-distance dispersal can be achieved through seed herbivory, mainly by roe deer (endozoochory), or through seeds being washed downslope from riparian habitats (hydrochory; Vittoz & Engler, 2007).

2.2 | Species occurrence data and pseudo-absence generation

From a total of 26 species occurrence databases (Appendix S1), we selected occurrences that were (a) only recently documented (post-2000), (b) of high precision (<100 m accuracy), and (c) from natural environments (no garden escapes or introduced individuals). The resulting 24,267 records were partitioned into spatially independent training and validation data, with a distance of at least 5 km between occurrences of the training dataset and occurrences of the validation dataset. Furthermore, each dataset was spatially thinned with a 10 km minimum distance between observations to avoid spatial autocorrelation. This distance was based on semi-variograms for each explanatory variable (Aiello-Lammens et al., 2015; Veloz, 2009). This resulted in seven training and validation subsets of 1,579 and 790 occurrences, respectively (see Figure 1 for an overview of the workflow). Filtering of available true absences (<100 m coordinate accuracy and post-2000 observation) resulted in a spatially biased dataset (Chytrý et al., 2016), and therefore, a presence-background approach was used. Background data were generated with spatial profiling (or geographic restriction) to (a) avoid false negatives, (b) exclude background data from areas outside of the species range, and (c) increase sensitivity (or the true-positive rate) of the modelling procedure (Barbet-Massin et al., 2012). More specifically, a spatial profiling range was determined ranging from 2.5 km distance from observed occurrences to 24.3 km, which was the maximum observed distance between occurrences in Europe. Spatially independent (10 km) background points were generated with 50%, 100% and 200% (maximum amount of spatially independent locations) of the presence dataset to test the effect of presence/background weighting on model performance (Barbet-Massin et al., 2012). Based on the area under the ROC curve (AUC) and the corrected Akaike information criterion (AICc), model performance peaked at 200% background points and all consecutive models were constructed accordingly. For validation of this approach, true absences were spatially thinned and spatially profiled on the extent of the Netherlands to test the accuracy of the presence-background modelling procedure.

2.3 | Explanatory variables

A total of 13 independent variables (Spearman $r < .6$) were included at 100 m resolution in the modelling procedure (Table 1; Appendix S2). Land use, elevation, aspect, degree of soil wetness and a river network map (Copernicus Land Monitoring Service et al., 2020) were included to model the effect of landscape-scale properties on the current species distribution (Lembrechts et al., 2018). The degree of soil wetness was based on the Water Wetness Probability Index (WWPI) and was determined independently from the vegetation cover. The river network database was transformed to an Euclidian distance raster, representing the distance of each cell (in metres) to the river features, and distances were $\log_{10}$-transformed. The landscape-level tree cover (originally at 1 km^2 resolution) of the three most important co-occurring tree genera (*Quercus*, *Carpinus*, *Fagus*) were also included (Brus et al., 2011). Physical properties of the soil ($n = 5$; Hiederer, 2013) were reduced in dimensionality with a Principal Component Analysis (PCA) to obtain two independent soil Principal Components (Table 2 of Appendix S2). To assess the trade-off between model complexity and variable importance, we used a backwards selection procedure based on AICc (Appendix S2). Selection of bioclimatic variables (WorldClim version 2.1; Fick & Hijmans, 2017) was based on the predictive capacity (AUC/AICc) of non-collinear combinations ($r < .6$; 1,077 models; Appendix S3), and three ecologically relevant and independent climatic variables were included

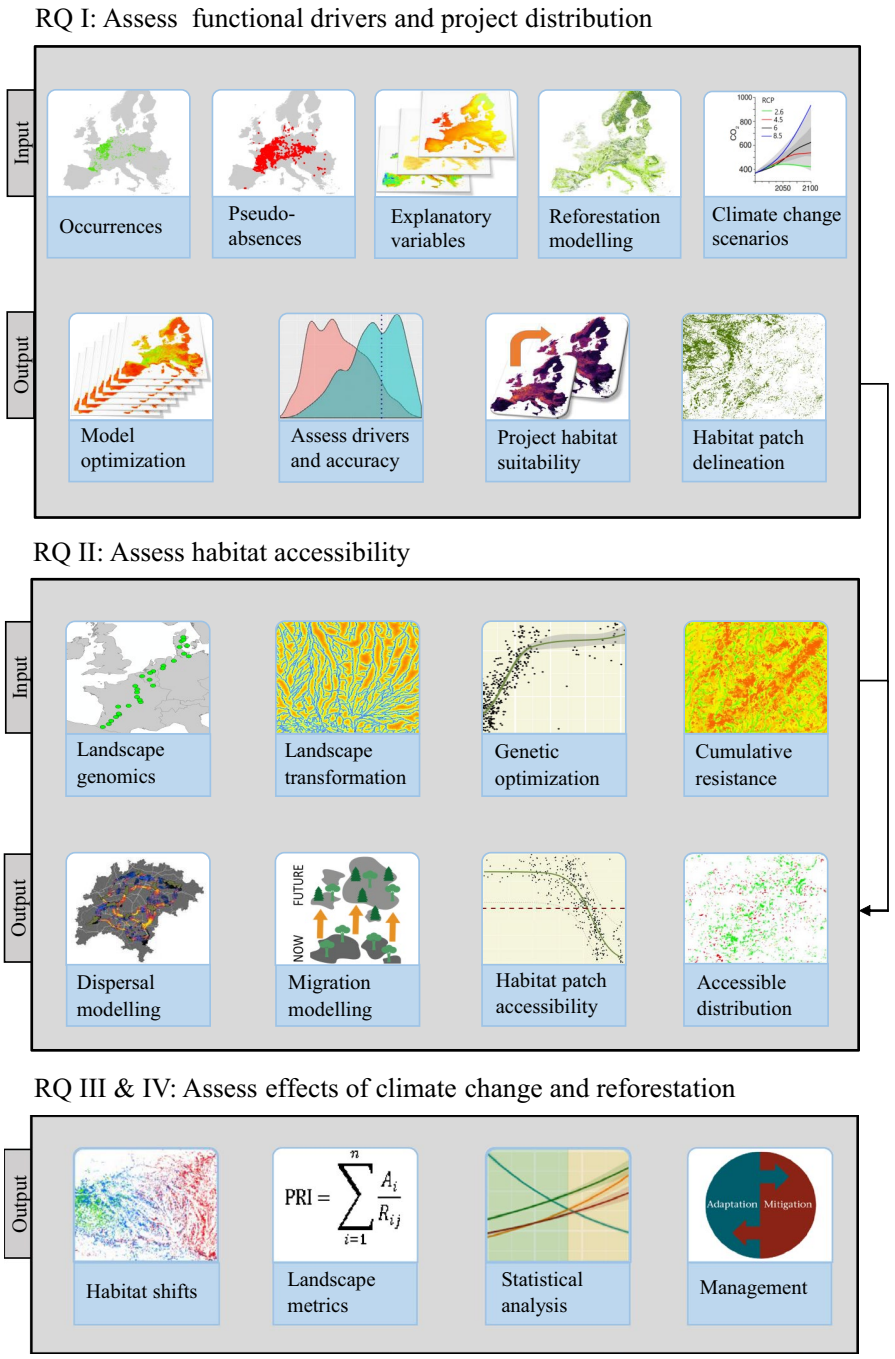

FIGURE 1 Workflow diagram

in the final model: temperature seasonality (Bio 4), precipitation of wettest month (Bio 13), and the precipitation of warmest quarter (Bio 18). Climate data, landscape-level tree species cover and soil data were disaggregated to 100 m resolution with bilinear interpolation to match the resolution of the other datasets (Fordham et al., 2012).

2.4 | Model building and projections

Nine distinct algorithms and ensemble models were evaluated on the extent of the Netherlands and a maximum entropy algorithm (Maxent) yielded the best results based on AUC. True absence Maxent models were compared with a presence/background strategy on the same extent and the latter performed better based on AUC and AICc (Appendix S4). The selection of nonlinear functions of environmental variables (features) and the settings of the regularization multiplier, which controls overfitting/complexity by regulating the chosen feature class intensity, are known to have a strong effect on Maxent predictions and should be carefully chosen (Merow et al., 2013). Parameterization of feature classes (linear, product, quadratic, hinge and threshold) and regularization multipliers were evaluated by ranking models (115 different parameter settings

TABLE 1 Mean variable contribution (± standard error) and variable permutation importance in the species distribution models ($n = 7$) of *Primula elatior* in Europe. CLC is the Corine land cover and WPI is the wetness proximity index as determined by the Copernicus Land Monitoring Service. Soil PC (1 and 2) are the first and second principal component axis from the soil physical properties as determined in Appendix S2

Feature	Contribution	Permutation Importance
CLC	54.05 ± 0.97	44.81 ± 1.08
Temperature seasonality	17.73 ± 0.48	17.81 ± 0.59
River distance (log_{10}-transformed)	13.79 ± 0.59	10.53 ± 0.24
Elevation	4 ± 0.33	8.64 ± 0.47
Precipitation of Warmest Quarter	3.45 ± 0.1	7.58 ± 0.24
Carpinus	1.9 ± 0.26	2.41 ± 0.32
Soil PC2	1.18 ± 0.15	1.34 ± 0.21
Quercus	1.09 ± 0.26	1.27 ± 0.26
Soil PC1	0.82 ± 0.09	2.09 ± 0.21
Fagus	0.71 ± 0.16	1.51 ± 0.22
Precipitation of Wettest Month	0.49 ± 0.07	0.95 ± 0.09
WPI	0.47 ± 0.13	0.53 ± 0.2
Aspect	0.32 ± 0.08	0.53 ± 0.09

tested on one data partition) according to AUC and AICc ("ENMeval v. 0.3.1"; Muscarella et al., 2014; Appendix S4). This parameter optimization method integrated the model complexity, inherent to the distinct features, and a combination of linear, product and threshold features were selected with a default (1) regularization multiplier as optimal parameters. The use of a default regularization multiplier is justified because we had a large amount of records, a diversity in the environmental data over the whole range, and less complex features than the default (Phillips & Dudík, 2008).

The resulting Maxent models were used to predict the relative suitability (presences relative to background data) for *P. elatior* in Europe for the current and projected climate (RO I), and for a forest restoration scenario (see section "Assessing mitigation effects of envisioned large-scale afforestation"). Bioclimatic projections according to three greenhouse gas scenarios in 2050, namely RCP 2.6, RCP 4.5 and RCP 8.5, were used to analyse future biogeographical shifts of the species distribution. RCP variables were based on averages from 11 general circulation models (Appendix S2).

Maxent's relative suitability output was transformed with a complementary log-log (cloglog) function to an estimate of occurrence probability ranging between 0 and 1 (Fithian et al., 2015; Phillips et al., 2017), and the resulting projections based on the 7 subsample datasets were averaged to obtain robust results. To determine a habitat suitability threshold for delineating suitable patches in an otherwise unsuitable landscape matrix (Nenzén & Araújo, 2011), we used the average projected probability (meanPred; see Appendix S5 for explored alternatives) of all 24,267 occurrences in our dataset (0.714; 95% CI [0.712, 0.715]). The meanPred threshold has been advised to reduce the false positive rate when species prevalence is moderate or high, which is essential to model dispersal between patches (Liu et al., 2013). All habitat above this threshold was considered suitable and patches were delineated based on connected cells according to the 8-neighbours rule (queen's case) with "landscapemetrics v. 1.5.1" (Hesselbarth et al., 2019). Thus, habitat patches are here defined as areas of suitable habitat consisting of contiguous cells with a minimum habitat suitability.

To validate the binary classification of patches, the true skill statistic (TSS) was calculated, which is based on the true-positive rate (TPR; within the habitat patch or an edge raster cell) of all occurrences and the true negative rate of a matching random sample of 24,267 absences (mean of 10 random absence generations). The TSS (TPR+TNR-1) ranges from −1 to 1, with values <0 indicating a performance which is no better than random (Allouche et al., 2006). Preprocessing was performed with the R package "raster v.3.0-7" (Hijmans, 2019), models were trained and projections obtained with "Maxent v. 3.4.3" (Phillips et al., 2020) using the R package "dismo v.1.1.4" (Hijmans et al., 2017), and evaluation was performed following Warren & Seifert (2011) with the R package "ENMeval v0.3.0" (Muscarella et al., 2014; Appendix S5) on the infrastructure of the Flemish Supercomputer Center (VSC; FWO, 2020).

2.5 | Modelling dispersal and migration events to determine the accessible area

We modelled potential dispersal and migration events based on circuit theory, which describes the landscape as a resistance matrix (cells on a geographical raster grid) and which determines multiple pathways of low resistance between suitable habitat patches (nodes). This measure of isolation between pairs of nodes was then expressed as effective resistance (McRae et al., 2008). Dispersal was here defined as seed movement between habitat patches within a specific scenario, thereby allowing functional connectivity between habitat patches. Migration was defined as repeated seed dispersal events across successive generations, thereby allowing functional connectivity between a current habitat patch and a habitat patch that will be present in the future (2050). The future patch accessibility was determined by both the potential for migration and the potential for dispersal between projected habitat patches (future isolation). The current patch accessibility was determined only by the dispersal potential (current isolation) under the assumption that the current projected distribution is stable and not yet affected by climate change. Because land use, distance to rivers and elevation were expected to affect seed dispersal probabilities in *P. elatior*, these variables were used to define the resistance matrix. For example, rivers were expected to facilitate dispersal and thus decrease the effective resistance, while anthropogenic land use and high elevation (upslope) was expected to increase the effective resistance. For elevation, the assumption was made that low resistance matrix values at low elevation were a proxy for downhill dispersal, and high resistance matrix values at high elevation were a proxy for uphill dispersal.

Because effective resistances are sensitive to user-specified resistance matrix values assigned to each environmental variable, a genetic optimization algorithm was applied to approximate the true cost of dispersal (see Appendix S6 for details on DNA sequencing and Appendix S7 for a detailed description of the genetic optimization of the resistance matrix). Briefly, this procedure determines the isolation by resistance (IBR) and is based on the expectation that a high effective resistance increases the genetic differentiation between populations under migration-drift equilibrium (McRae, 2006). Specifically, we sampled leaves from 10 individuals in each of 29 *P. elatior* populations along a latitudinal gradient from southern France to Northern Denmark. Only large, connected habitats were sampled to exclude populations in non-equilibrium states. We used single nucleotide polymorphism (SNP) skimming (Wessinger et al., 2018) to construct SNP matrices containing 406 pairwise Nei's genetic distances (Nei, 1978). The SNP matrix was constructed with the R packages "adegenet v.2.1.2", "vcfR v.1.8.0", "tidyverse v.1.2.1" and the genetic distances were calculated with "stAMPP v.1.6.1". These 29 populations captured variation in land use and river distance but not in elevation. To nevertheless account for elevation as a potential dispersal-inhibiting factor, we retrieved genetic data from Konečná et al. (2019), who evaluated colonization of subalpine habitats in central European mountains by *P. elatior*. This dataset contains a pairwise F_{st} matrix for 16 populations or 120 pairwise distances and was used to separately optimize the resistance matrix of elevation. The genetic optimization (232 models; Appendix S7) was based on the log-likelihood rank of standardized maximum-likelihood population-effects (MLPE) mixed models, using genetic distance as the response and $\log_{10}$-transformed effective resistance as the predictor (Clarke et al., 2002). Additionally linearized partial Mantel tests were used, removing the effect of $\log_{10}$-transformed Euclidean distance from the $\log_{10}$-transformed effective resistance (Cushman et al., 2006). The distinct genetically optimized resistance matrices (land use, distance to rivers and elevation) were parameterized by iteratively assigning weights (from 0.1 to 1) to each resistance matrix (110 models), resulting in a new resistance matrix which was then used for connectivity analysis (Koen et al., 2012). The resistance matrices for the projected forest restoration scenarios were adapted to reflect the genetically optimized land use resistance matrix (Appendix S7). Effective resistances were calculated using "Circuitscape v5.5.5" (McRae & Shah, 2011) in "Julia v1.3.1" (Anantharaman et al., 2019) on the Flemish Supercomputer infrastructure (VSC; FWO, 2020). Resistance matrix optimization and MLPE models were executed with the R packages "ResistanceGA v.4.0-14" (Peterman, 2018) and Mantel statistic derivatives were constructed with "Vegan v.2.5-5".

We modelled whether dispersal between habitat patches could take place as a function of the effective resistance between them. Because suitable habitat patches can either function as sources for further dispersal (stepping stones or source patches) or dispersal dead-ends, we also quantified the within-patch dispersal potential for each suitable patch based on the effective resistance between patch edge and patch centroid. Habitat patches where within-patch dispersal from edge to centroid is highly unlikely (dispersal dead-ends) were then excluded as source patches or stepping-stones. Migration potential was then quantified based on the effective resistance between currently suitable source patches and projected suitable habitat patches in 2050 (see Appendix S8 for the effect of source patch exclusion on migration probabilities). The potential for dispersal (between and within habitat patches) and migration was based on the isolation by resistance relationship. The sigmoid isolation by resistance relationship (Figure 2) was determined by a self-starting nonlinear least square model with the genetic similarity as response and the logarithmic effective resistance as predictor. Genetic similarity was defined as a function of Nei's genetic distance (y) and ranges between 1 and 100:

$$\text{Genetic similarity} = \left(1 - \frac{(y - \min(y))}{\max(y) - \min(y)}\right) \times 100$$

The isolation by resistance model was used to predict genetic similarities based on the calculated effective resistances for dispersal

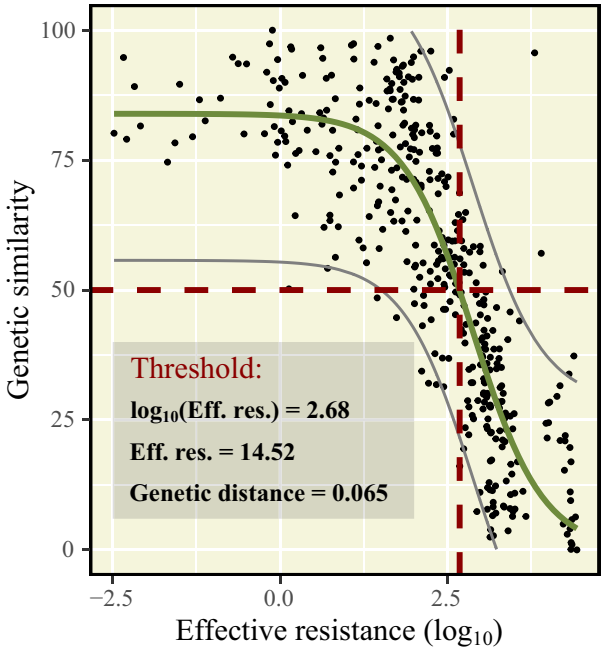

FIGURE 2 Sigmoid isolation by resistance relationship between the genetic similarity and the $\log_{10}$-transformed effective resistance (see Appendix S7 for the untransformed relationship with genetic distance) of *Primula elatior* in Europe. Genetic similarity is a function of Nei's genetic distance and ranges between 1 and 100 with high values indicating high similarity. This isolation by resistance relationship determines the dispersal potential, migration potential and the accessibility of habitat patches. Dispersal limitation takes place at effective resistance values where the slope starts to decrease ($\log_{10}$-transformed effective resistance of approx. 1.25). The threshold (dashed red line) is defined at the centre of the sigmoid curve (inflection point) where the decrease in genetic similarity is at its highest point and dispersal limitation is certain. The linear decrease of genetic similarity at the higher end of the $\log_{10}$-transformed effective resistance (right side of the *x*-axis) suggests a migration–drift equilibrium (Van Strien et al., 2015)

and migration in each species distribution scenario. The dispersal and migration potential thus reflect their respective predicted genetic similarities. Dispersal limitation takes place at logarithmic effective resistance values where the genetic similarity starts to decrease and is certain at the centre of the sigmoid curve (inflection point). A binary accessibility metric for dispersal and migration was based on this inflection point and corresponds to a genetic similarity of 50, an effective resistance of 14.52 and a genetic Nei's distance of 0.065. A patch was thus considered accessible when the dispersal and migration potential exceeded a genetic similarity of 50 (see Appendix S7 for a detailed evaluation of this threshold). To demonstrate how dispersal affects the projected distribution, we calculated (a) the total area of suitable habitat (TA); (b) the suitable area that is so isolated that dispersal is unlikely to take place (dispersal-limited area: DLA); (c) the suitable area where the colonization capacity is restricted due to within-patch dispersal limitation (WLA); (d) the suitable area that is not accessible through migration (migration-limited area: MLA); and (e) the suitable area that is accessible (AA). The accessible area in a specific scenario is thus determined by the dispersal-limited area and the migration-limited area (AA = TA−{DLA + MLA}), and the migration-limited area is determined by the within-patch dispersal limitation of the current distribution (RO II). DLA, WLA, MLA and AA are determined by the before mentioned isolation by resistance threshold.

2.6 | Assessing shifts in patch distribution and configuration

To assess shifts in the patch distribution, we evaluated the median latitude, continentality (distance from the sea) and elevation with non-parametric Kruskal–Wallis tests. Pairwise comparisons between scenarios were evaluated with a Wilcoxon rank sum test (Mann–Whitney) with a Benjamini and Hochberg (1995) adjustment of the p values. Uncertainty was determined with the 95% confidence interval of the median.

Generalized linear models were used to determine to what extent climate change affects the patch accessibility and proximity resistance index (PRI) across space and time (RO III) with the following model:

$$\text{Response} \sim \text{RCPScenario} \times \text{Latitude} + \text{RCPScenario} \times \text{Continentality}$$

Patch accessibility is a binary metric determined by the dispersal and migration potential, as explained in the last section. The PRI is an index accounting for patch size, similar to the patch proximity index proposed by Gustafson and Parker (1994), but with nearest-neighbour patch distance replaced by the effective resistance. The PRI is an indicator of metapopulation dynamics, with high values indicating stable metapopulations (Gustafson & Parker, 1994). The PRI value of a habitat patch was calculated by identifying each habitat patch (*i*) whose edge lay at least partially within the proximity buffer (5,000 m) of the focal patch centroid being indexed. The PRI was calculated based on the area in hectares (*A*) and the edge-to-edge effective resistance of dispersal (*R*) from patch *i* to its nearest neighbour:

$$\text{PRI} = \sum_{i=1}^{n} \frac{A_i}{R_i}$$

RCP Scenario represents a categorical variable indicating the respective climate change pathway (3) versus the current distribution (intercept). Climate change impacts within scenarios were assessed by their interaction effects with patch latitude and continentality. Significant interaction effects of the respective climate scenarios with latitude and continentality indicate shifts in patch accessibility and the PRI within a projected future distribution, compared to the current projected distribution (intercept). A binomial error distribution family with a logit link function was used to model accessibility and a Gaussian error distribution with $\log_{10}$-transformation of the response was used to model the PRI. The minimum latitude was set as the most southern patch and was therefore corrected for in the models by subtracting the minimum latitude from each coordinate. The generalized linear model with PRI as response was weighted to correct for heteroscedasticity. The weights were determined based on a linear model of the unweighted model residuals as explained by the unweighted predicted values (absolute model residuals ~ predicted values). The predicted weights were then transformed (1/predicted weights^4) and used as input for the weighted model. Model results were presented by the predicted scenario means and their respective standard error, while the uncertainty interval in the figures was presented with the 95% confidence interval. Overall effects are depicted by the mean and standard deviation of climate scenarios (3). The proportion of deviance explained in the models was determined by the D^2 adjusted with "modEvA v2.0" in R (Guisan & Zimmermann, 2000). The explained variance of each fixed term (scenario, geographic components and their interaction) was partitioned to disentangle climate change effects from geographic effects. A more in depth analysis of explained variance drivers, regional effects, the relative contribution of area and dispersal probabilities to PRI, and the relative contribution of dispersal and migration probabilities to patch accessibility can be found in Appendix S8.

2.7 | Assessing mitigation effects of envisioned large-scale afforestation

To analyse the potential mitigation effect of anticipated forest restoration targets in the EU, we constructed a land use change scenario based on the observed 0.4% annual total forest gain in the past decades (European Commission, 2013). This projected forest gain is in line with EU policy targets aiming to plant 3 billion trees per decade, and the expected natural regeneration on abandoned farmland (European Commission, 2020). To this end, variable buffers were constructed surrounding the Corine (CLC) broadleaf forests (400 m), mixed forests (100 m) and coniferous forests (200 m), and an intersect of each separate layer was taken with the LUISA

forest reference scenario, which depicts the projected land use change by 2050 (Lavalle, 2014). This approach enables refining broad coarse scale projections for forest change to specific forest types and predicts a total forest gain of 12% (19 million hectares) between 2020 and 2050 (0.4% annually). Due to predicted massive mortality events of coniferous species by the end of the century (McDowell et al., 2016), forest restoration efforts are likely to be focused on broadleaf species (Spiecker et al., 2004). Therefore, our forest restoration scenario (from here on referred to as "2050 mitigation") corresponds to a partial broad-leaved forest increase of 55.9% and a mixed and coniferous forest decrease by 19.2% and 8.1%, respectively.

The mitigating effect of reforestation on patch latitude and continentality was based on non-parametric pairwise comparisons (Wilcoxon rank sum/Mann–Whitney test) of scenario medians. To assess to what extent reforestation can mitigate climate change impacts of patch accessibility and PRI, we evaluated the following models (RO IV):

$$\text{Response} \sim \text{RCPScenario} \times \text{Mitigation}$$

Mitigation was a binary categorical variable that determines whether the species distribution model for 2050 was created using the baseline land use or using the reforestation land use scenario.

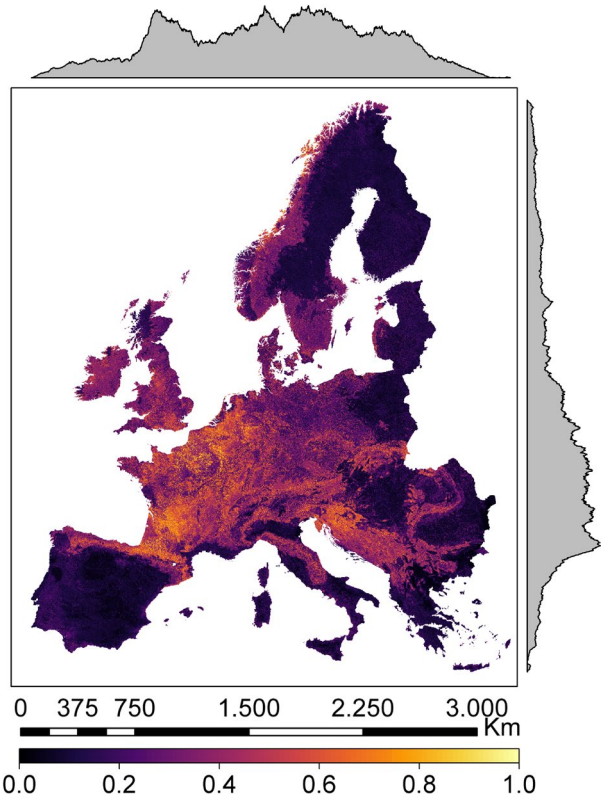

FIGURE 3 Predicted suitability of *Primula elatior* in Europe. The density curve displays the cumulative suitability as a function of latitude (y) and longitude (x). The predicted suitability ranges from 0 to 1 and is displayed in the colour key bar

3 | RESULTS

3.1 | Drivers of the habitat suitability and distribution

The predicted suitability for *P. elatior* is high from the foot of the Pyrenees and throughout the Atlantic zone, but decreases towards Denmark (Figure 3). Furthermore, suitability hotspots can be observed near Slovenia and continental Croatia and in the northwestern maritime zone of Norway. Introduced populations which thrive well in Norway were generally correctly identified as suitable hotspots. The mean AUC of the predicted suitability was 0.81 (Figure 3 in Appendix S5). The true-positive rate (TPR) of all occurrences in relation to predicted suitable habitat patches was 0.68, the true-negative rate (TNR) was 0.96 and the resulting true skill statistic was 0.64.

Landscape-scale and macro-climatic variables contributed 78.33% and 21.67%, respectively, to the model (RO I; Table 1). Land use was the main predictor of *P. elatior* occurrences in Europe, where broad-leaved forest, mixed forest, green urban areas and agriculture with a considerable amount of natural vegetation had a clear positive effect on the projected distribution (Figure 1 in Appendix S5). Occurrences could generally be observed in areas with an intermediate temperature seasonality (annual temperature variability) and the niche optimum ranged from 4.12 to 6.62℃ (>.5 probability of presence) standard deviation (Figure 2 in Appendix S5). The probability of occurrence sharply declined below 250 mm of rainfall during the warmest quarter. The negative relation of the species' occurrence to the $\log_{10}$-transformed distance to rivers and elevation reflected its association with riparian zones and lowlands. Although soil physical properties (Soil PC1 and PC2), landscape-level tree species cover (*Carpinus*, *Quercus and Fagus*), orientation (aspect) and degree of soil wetness (WPI) significantly affected model accuracy (>Δ2 AICc), their contribution was limited.

The projected increase in temperature seasonality and decrease in rainfall during the warmest quarter by 2050 is expected to result in a total net loss (RO I) of 17,721 km^2 suitable habitat (−31.2%) under RCP 2.6, 23,587 km^2 (−49.4%) under RCP 4.5 and 26,036 km^2 under RCP 8.5 (−58.5%). Overall, the projected change in habitat suitability due to climate change was estimated to result in the loss of 46.4 ± 13.9% (mean ± *SD* of climate change scenarios) of currently available habitat. However, the actual colonisation of new suitable habitat in 2050 depended on the dispersal capacity of the species.

3.2 | Accessibility of suitable habitat through dispersal and migration

Land use, river distance and elevation contributed 45.5%, 36.4% and 18.2%, respectively, to the resistance matrix, and effective resistances had a high explanatory power for genetic distance (MLPE:

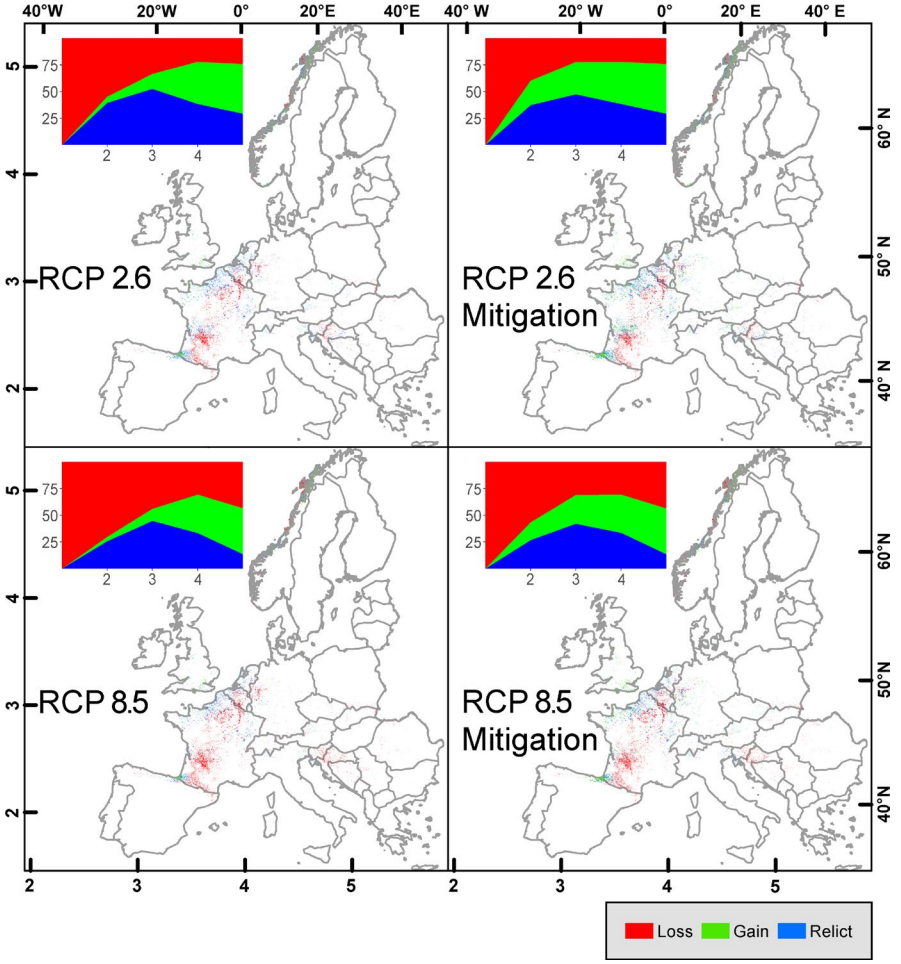

FIGURE 4 Habitat loss (red), gain (green) and habitat relicts (unchanged; blue) of *Primula elatior* in Europe for RCP 2.6 and RCP 8.5, with (right) and without (left) forest restoration mitigation. Dispersal and migration limitations are taken into account for the displayed habitat change. All geographical calculations are based on the ETRS89-extended/LAEA Europe and the scale is visualized in 10^6 metres on the left (latitude) and on the bottom (longitude). WGS84 graticules are indicated in degrees (curved projection) on the right (latitude) and on the top (longitude). The embedded figures display the proportional turnover (%) of habitat in loss, gain and relict (unchanged habitat), respectively (*y*-axis) in relation to the latitude (*x*-axis) in 10^6 metres (LAEA Europe)

$R^2_{marginal}$ = .76, $R^2_{conditional}$ = .92, and the partial Mantel statistic was 0.77). The predicted accessibility of habitat patches decreased from 94.1% (current projected distribution) to 72.6% for RCP 2.6, to 72.8% for RCP 4.5 and to 70.3% for RCP 8.5 (*SE* < 0.1 in all scenarios). The low migration potential resulted in a reduction of the accessible distribution area (RO II) in all scenarios, where 33,510 km^2 (−40.2% compared to the current scenario) of the projected distribution area was accessible for RCP 2.6 compared to 28,274 km^2 (−49.5%) for RCP 4.5 and 23,735 km^2 (−57.6%) for RCP 8.5 (Figure 4; Figure 5). The limited migration potential thus resulted in 15.6 ± 1.7% (mean ± *SD* of climate change scenarios) of the projected total distribution in 2050 that was not accessible.

3.3 | Expected shifts in the habitat distribution and configuration

Projected habitat loss was most severe in continental France, and habitat gain was most prevalent in the temperate maritime climate zones of France, England and Norway (Figure 4). The median latitude of suitable habitat patches shifted northwards by 148.8 ± CI [144.8, 153.2] km for RCP 2.6, 182.4 ± CI [178.8, 186] km for RCP 4.5 and 218.4 ± CI [214.8, 222.4] km for RCP 8.5 relative to the current median latitude of 2.752 × 10^6 ± CI [2.747, 2.756] m (chi-square = 8,494.8, *p* = <.001, *df* = 6). The median distance from the sea of suitable habitat patches (i.e. their continentality) decreased by 48.8 ± CI [47.5, 50] km for RCP 2.6, 58.1 ± CI [56.7, 59.3] km for RCP 4.5 and 67.4 ± CI [66.3, 68.6] km for RCP 8.5, relative to the current median distance of 124.9 ± CI [123.4, 126.5] km (Chi square = 3,309.1, *p* = <.001, *df* = 6). Surprisingly, the median elevation of suitable patches decreased by 45.1 ± CI [42.8, 47.7] m for RCP 2.6, 52 ± CI [49.6, 54.7] m for RCP 4.5 and 63.6 ± CI [61.1, 61.1] m for RCP 8.5 relative to the current median elevation of 200.7 ± CI [198.3, 203.4] m (chi-square = 2,638.6, *p* = <.001, *df* = 6). However, the reduction in median elevation was most likely related to the shift to a more maritime climate and was therefore not considered further (Appendix S8).

The distribution shift of habitat patches resulted in a reduced patch accessibility in the north and in the more temperate maritime regions (RO III; Table 2; Figure 6). The predicted average PRI of accessible habitat patches decreased from 210.4 in the current projected distribution to 158.3 for RCP 2.6, 116.1 for RCP 4.5 and 118.2 for RCP 8.5, with a standard error smaller than 0.1 for each scenario. Furthermore, the PRI strongly decreased in the south under climate change (see Table 2 for test statistics and Figure 6 for predicted means and their confidence interval).

Overall, the median latitude of habitat patches is thus expected to shift 183.2 ± 34.8 km (mean ± *SD* of climate change scenarios)

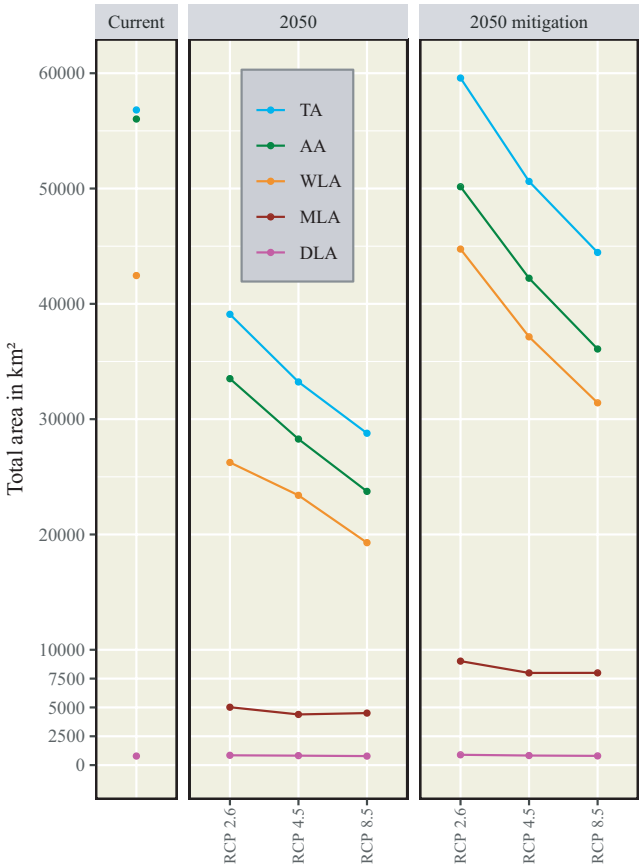

FIGURE 5 Scenario-specific summaries of the projected total distribution area (TA), accessible area (AA), within-patch dispersal-limited area (WLA), migration-limited area (MLA) and dispersal-limited area (DLA) of *Primula elatior* in Europe

northwards and 58.1 ± 9.3 km (mean ± *SD*) to more maritime climate regions. Furthermore, the PRI is expected to reduce by 37.8 ± 11.3% (mean ± *SD*) under climate change.

3.4 | Mitigation effects of large-scale afforestation

Reforestation mitigated 115.6% (net gain) of the total distribution area loss for RCP 2.6, 73.7% for RCP 4.5 and 55.9% for RCP 8.5. The mitigation of the accessible distribution area loss amounted to 73.9% for RCP 2.6, 50.3% for RCP 4.5 and 38.2% for RCP 8.5 (RO IV). The median northward latitudinal shift was only slightly mitigated for RCP 2.6 (1.3% reduction; $p = .037$) and not significantly mitigated for RCP 4.5 (5.9%, $p = .108$). However, 6.9% of the median northward shift was mitigated for RCP 8.5 ($p = <.001$). The median predicted shift from continental to more maritime regions was considerably mitigated, with a 35.6% reduction for RCP 2.6 ($p = <.001$), 34.8% reduction for RCP 4.5 ($p = <.001$) and 30.0% reduction for RCP 8.5 ($p = <.001$; see Appendix S8 for post hoc result tables and an overview of scenario medians and their 95% confidence intervals).

Overall, reforestation mitigated 81.7 ± 30.7% (mean ± *SD* of climate change scenarios) of the total distribution area loss, 54.1 ± 18.2% (mean ± *SD*) of the accessible habitat area loss and 33.5 ± 3% (mean ± *SD*) of the shift in the median habitat patch continentality. More habitat became available in the north and more maritime regions under reforestation management (Figure 5 and Appendix S8). Therefore, the predicted mean (±*SD*) patch accessibility decreased in 2050 to 65 ± 0.9% compared to 72 ± 1.5% without reforestation management (Figure 7). However, reforestation mitigated 49.5 ± 4.2% (mean ± *SD*) of the loss in PRI in the accessible distribution area due to climate change (see Table 2 for test statistics and Figure 7 for predicted confidence intervals).

4 | DISCUSSION

4.1 | Suitability drivers

The high contribution of landscape-scale variables in our species distribution model, with land use, distance to rivers and elevation as main predictors, points at the importance of ecosystem characteristics and landscape-scale processes for the occurrence of *P. elatior*. The importance of distance to rivers confirms its known ecological niche of rich mesic soils with loam deposits and high organic matter content, typical of floodplain forests (Taylor & Woodell, 2008). Furthermore, the importance of local and landscape-scale conditions for the occurrence of *P. elatior* is in line with other studies examining such drivers on forest herbs (Bernhardt-Römermann et al., 2015; Greiser et al., 2020; Valdés et al., 2015). Even though local factors are important drivers, climate still has a considerable contribution to the species' distribution (21.7%). A clear optimum in temperature seasonality implies a dependence on annual variation in temperatures, but also a sensitivity to temperature extremes. This coincides with earlier findings that exposed a strong phenological sensitivity in *P. elatior* (Baeten et al., 2015). The positive relation between the precipitation of the warmest quarter and *P. elatior* occurrences confirms the intolerance to desiccation of the species (Whale, 1983). Climate change effects are projected to be more severe in southern continental regions (Fick & Hijmans, 2017), and therefore, it is likely that conditions would shift outside of the species' climatic niche optimum in these regions. In the more maritime and northern regions, on the other hand, new available habitat is likely to become available because the climatic niche would shift into the species' optimum (Figure 4). Expected habitat loss in the continental south exceeds habitat gain in northern and maritime regions and the total distribution area is likely to reduce considerably by 2050 (46.4 ± 13.9%; mean ± *SD*). This coincides with the coarse median suitability loss of forest herb flora distributions in Europe predicted by Skov and Svenning (2004). However, one limitation of our study is that we did not take the climatic buffering effect of forests directly into account (Lembrechts et al., 2018; Zellweger et al., 2020). Furthermore, species responses to macro-climatic changes might be attenuated by plant phenotypic responses and/or local adaptation of fitness-related traits (Benito Garzón et al., 2019; Razgour et al., 2019). Integrating both temperature measurements of forest and riparian microclimates, and the adaptive potential of populations in predictions could further improve accuracy in the future.

TABLE 2 Climate change effects on the accessibility and proximity resistance index (PRI) of projected *Primula elatior* habitat patches in Europe. "Between scenario" climate change effects are determined by the projected scenario (factor), geographic effects are determined by latitude and continentality (continuous) and the distribution shifts (within scenario) are determined by the interaction of geographic effects with scenario's. *N* depicts the total amount of projected habitat patches in each scenario and values correspond to z-statistics (Accessibility) and t-statistics (PRI) of the fixed terms. Effects on patch accessibility (binary) are based on the total distribution area and the proximity resistance index (PRI) is based on the accessible area. The intercept is the current scenario and the minimum latitude is corrected to the most southern patch (latitude−min{latitude}). Residual variance is largely related to regional differentiation in observed patterns (Appendix S8). The reforestation section depicts the overall mitigation effect and the scenario-specific mitigation effects are determined by the interaction between climate change scenario and a reforestation factor (binary). The intercept depicts the corresponding climate change scenario without reforestation. Each row and each column in the reforestation section corresponds to a distinct model and the intercept corresponds to the overall mitigation model. Scenario-specific mitigation effects are calculated on data subsets (future scenario with and without reforestation)

Term	*N*	Accessibility	PRI	Effect
Intercept (Current)	57,840	73.8***	164.3***	Between scenario
RCP 2.6	51,000	−33.8***	−22.3***	
RCP 4.5	43,989	−32.4***	−32.4***	
RCP 8.5	39,879	−32.3***	−27.2***	
Latitude		−21.7***	−40.6***	Geographic
Continentality		−12***	−58.6***	
RCP 2.6 × Latitude		−8.5***	21.4***	Within scenario (shift)
RCP 4.5 × Latitude		−8.2***	27.1***	
RCP 8.5 × Latitude		−10.5***	21.8***	
RCP 2.6 × Continentality		22.4***	−5.5***	
RCP 4.5 × Continentality		21.6***	−0.6	
RCP 8.5 × Continentality		23.2***	2.1*	
Explained variance (D^2_{adj})		15	11.7	Variance partitioning (%)
Scenario		46.7	16.3	
Interaction (shift)		4.0	3.1	
Climate change		50.7	19.4	
Geographical		49.3	80.6	
Intercept (Climate change)		99.2***	572.3***	Reforestation
RCP 2.6 × mitigation	57,606	−26.2***	13.9***	
RCP 4.5 × mitigation	51,354	−22.1***	27.6***	
RCP 8.5 × mitigation	47,547	−18.3***	18.1***	
Overall mitigation	+7,213 ± 316	−26.2***	14***	

***$p \leq .001$.; **$p \leq .01$; *$p \leq .05$.

4.2 | Predicting spatio-temporal dispersal patterns

Due to the low predicted migration potential of *P. elatior* to new available habitat in 2050 (Figure 5), it is estimated that 15.6 ± 1.7% (mean ± *SD*) of the projected total distribution area will be inaccessible for colonization. The low migration potential of *P. elatior* is reflected by its inherent life-history traits, such as the long period until first reproduction (~3 years), specific germination requirements and absence of specific dispersal mechanisms (Taylor & Woodell, 2008; Verheyen et al., 2003). Honnay et al., (2002) and Jacquemyn et al., (2002) both empirically determined the dispersal potential of *P. elatior* in fragmented landscapes and found that colonization after 40–50 years was virtually zero when habitat patches were more than 1,000 m apart. This roughly coincides with modelled dispersal rates of 24 to 95 m per year in forest species without adaptations to animal dispersal vectors (Dullinger et al., 2015). Correspondingly, the mean migration distance of accessible *P. elatior* patches in our future scenarios is 481 ± 3 m (mean ± *SE*), while non-accessible patches have on average a 10,015 ± 49 m (mean ± *SE*) distance (Appendix S7). Source populations should thus be able to colonize newly available patches if they disperse on average 16 m per year over a 30-year timeframe.

One limitation in using effective resistance to model migration patterns is the inability to integrate gradual landscape changes. New algorithms that calculate stepwise dispersal between intermediate scenarios could improve biological realism (Engler et al., 2012), but this process would further complicate the genetic optimization process. In addition, efforts that link field-verified colonisation rates over time (e.g. individual-based spatially explicit modelling; Landguth et al., 2010) with genetic divergence could improve the temporal estimation of dispersal models. Taking these limitations in account, our study integrates the genetic and landscape structure on a continental scale which results in highly accurate isolation-by-resistance predictions on a habitat patch scale. The functional dispersal patterns of *P. elatior* emphasize the importance of streams as efficient corridors

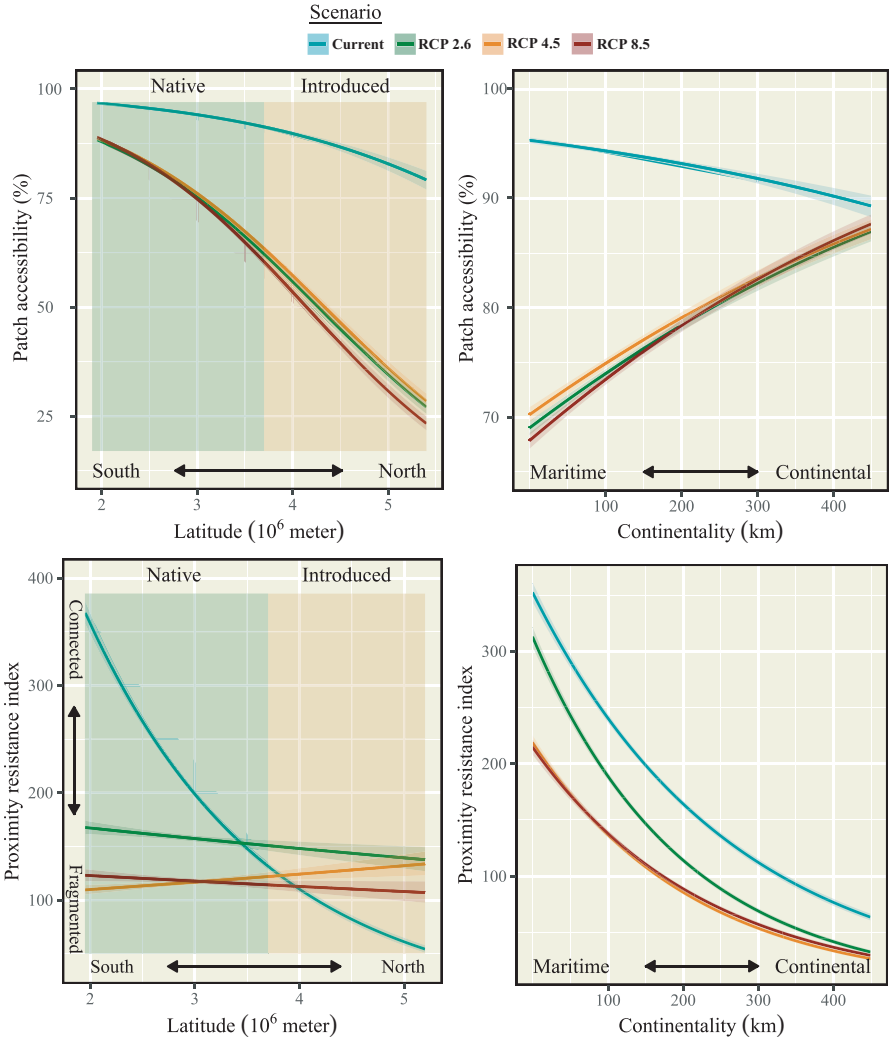

FIGURE 6 Interaction effects between climate change (scenario) and the geographical position of *Primula elatior* habitat patches (as determined by latitude and continentality) on patch accessibility and the proximity resistance index. The predicted means and their 95% confidence interval (colour fill) relate to the within-scenario effects in Table 2. The latitude is represented in meters based on the LAEA89 coordinate system and continentality is represented in km distance from the coast. The patch accessibility is based on the total distribution area and the proximity resistance index is based on the total accessible area. The northernmost known native populations (green) can be found around 3.7×10^6 m latitude (LAEA89) or 57° North (WGS84). More northern populations in Norway (beige) are known to have been introduced and are therefore marked separately

(Araujo Calçada et al., 2013) and the modelled dispersal of *Primula elatior* could extend to other perennial herb species that often occur in alluvial forests and are slow colonizers such as *Lysimachia nemorum*, *Lamium galeobdolon*, *Anemone nemorosa*, *Paris quadrifolia*, *Circaea lutetiana*, *Arum maculatum*, *Chrysosplenium alternifolium*, *Allium ursinum*, and *Chrysosplenium oppositifolium* (Verheyen et al., 2003). Validation of our approach for these and other forest herbs could further optimize management decisions to protect and restore forest understorey communities in a context of global change.

4.3 | The impact of climate change on habitat distribution and configuration

Climate change will likely result in a northward shift of the median patch distribution (183.2 ± 34.8 km; mean ± *SD*) and to more maritime regions (58.1 ± 9.3 km; mean ± *SD*). The low migration potential to new available habitat is estimated to result in a general reduction of patch accessibility in these regions (Figure 6 and Appendix S8). This indicates that *P. elatior* will not be able to track the changing climate, which is in line with research of other understorey herbs (Dullinger et al., 2015; Honnay et al., 2002; Takahashi & Kamitani, 2004). Not the least because the North Sea and a non-suitable region in Sweden separates the fragmented populations at the leading edge from the newly available maritime habitat in Norway. The significant reduction of available projected habitat in the continental south by 2050 (Figure 5) and decrease in dispersal probabilities between habitat patches (Appendix S8) will likely cause a general reduction of the metapopulation stability (as determined by PRI) in these regions (Table 2; Figure 6). *P. elatior* is known to quickly lose genetic diversity when the metapopulation stability decreases (Jacquemyn et al., 2009), and therefore, southern remnant populations are estimated to still be threatened in the long term.

Interestingly, populations that were introduced in Norway during the late 19th century are currently in the naturalisation process (Gederaas et al., 2012). The ten regions currently occupied there, are in the close vicinity of habitat gain in the future, and could drive local migration patterns. Therefore, current naturalizing populations could become part of the shifting range. Overall, this illustrates the value of our modelling strategy for guiding assisted migration scenarios (Hunter-Ayad et al., 2020). Combining SDMs with dispersal models thus have a strong potential for guiding conservation and restoration efforts, but field validation remains critical (Laliberté & St-Laurent, 2020).

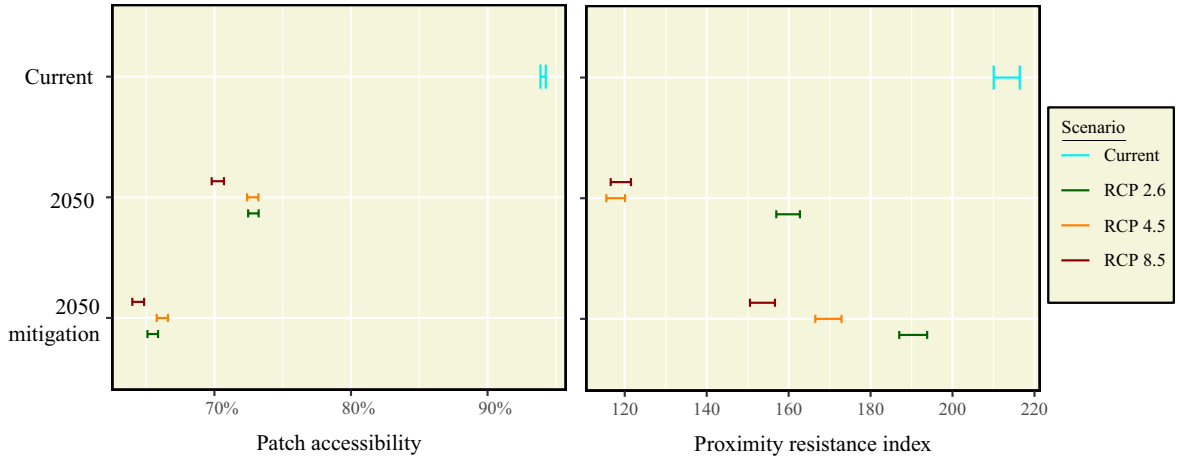

FIGURE 7 Predicted 95% confidence intervals of habitat patch accessibility and metapopulation stability, as determined by the proximity resistance index (PRI). The Y-axis depicts the projected current distribution ("Current") of *Primula elatior*, the projected distribution in 2050 under climate change ("2050") and the projected distribution in 2050 under climate change with large-scale reforestation/afforestation ("2050 mitigation"). The predicted mean and confidence intervals relate to the GLM models used to assess mitigation effects of reforestation with RCP Scenario × Mitigation as explanatory variable

4.4 | Mitigating climate change effect of forest herbs

Reforestation will likely mitigate most of the projected habitat loss due to climate change (81.7 ± 30.7%; mean ± *SD*) and a substantial amount of the accessible habitat area loss (54.1 ± 18.2%; mean ± *SD*). The mitigation of the shift in the median patch latitude is limited because mitigating effects in the south of the range are accompanied by habitat gain in the north of the range (Figure 5). Therefore, patch accessibility is not positively affected by reforestation. However, habitat gain in continental regions in the centre of the distribution (Figure 5) results in a considerable mitigation of the median patch continentality shift. These areas are generally in the vicinity of existing populations and are therefore accessible for migration. Habitat gain in the vicinity of these remaining populations results in a considerable mitigation of the loss in metapopulation stability (49.5 ± 4.2%; mean ± *SD*), as determined by the PRI. However, it is important to note that colonization success of reforested and afforested habitat patches is strongly dependent on past land use patterns. Successful colonization is often delayed by decades to centuries and short-term mitigation effects could therefore turn out to be lower than anticipated (Baeten et al., 2010; Naaf & Kolk, 2015).

5 | CONCLUSION

The sensitivity of *Primula elatior* to the change in seasonal climate patterns and rainfall during the warmest quarter will likely result in a considerable loss of the total distribution area by 2050. Furthermore, due to its limited migration capacity, it is estimated that the species will be unable to track the shifting climate. The metapopulation stability will likely decrease across the range and southern populations will be most affected. Reforestation is estimated to considerably mitigate the loss of the distribution area, and metapopulations are predicted to remain more stable. However, to completely alleviate habitat loss it seems required to integrate strategies for climate change mitigation (RCP 2.6), reforestation, restoration of ecological connectivity and assisted migration.

ACKNOWLEDGEMENTS

This research was funded by the Flemish Research Foundation (FWO project G091419N). Genetic data were collected in accordance with the Nagoya protocol on access to genetic resources (NOR: TREL1902817S/128). We would like to thank local biodiversity agencies for providing occurrence data. Furthermore, we would like to thank Koenraad Van Meerbeek for useful comments.

CONFLICT OF INTEREST

The authors declare that they have no conflict of interest.

PEER REVIEW

The peer review history for this article is available at https://publons.com/publon/10.1111/ddi.13367.

DATA AVAILABILITY STATEMENT

Training and validation data for the species distribution modelling, projections across space and time, the isolation by resistance model and corresponding data, and shapefiles containing patch-specific characteristics are deposited in a Dryad data repository: https://doi.org/10.5061/dryad.msbcc2fxx.

ORCID

Frederik Van Daele https://orcid.org/0000-0001-5827-722X
Olivier Honnay https://orcid.org/0000-0002-4287-8511
Hanne De Kort https://orcid.org/0000-0003-2516-0134

REFERENCES

Aiello-Lammens, M. E., Boria, R. A., Radosavljevic, A., Vilela, B., & Anderson, R. P. (2015). spThin: An R package for spatial thinning

of species occurrence records for use in ecological niche models. *Ecography*, *38*(5), 541–545. https://doi.org/10.1111/ecog.01132

Allouche, O., Tsoar, A., & Kadmon, R. (2006). Assessing the accuracy of species distribution models: Prevalence, kappa and the true skill statistic (TSS). *Journal of Applied Ecology*, *43*(6), 1223–1232. https://doi.org/10.1111/j.1365-2664.2006.01214.x

Alm, T. P., & Often, A. (2009). Centaurea phrygia subsp. phrygia as a German polemochore in Sor-Varanger, NE Norway, with notes on other taxa of similar origin. *Botanische Jahrbücher Für Systematik, Pflanzengeschichte Und Pflanzengeographie*, *127*(4), 417–432. https://doi.org/10.1127/0006-8152/2009/0127-0417

Anantharaman, R., Hall, K., Shah, V., & Edelman, A. (2019). Circuitscape in Julia: High performance connectivity modelling to support conservation decisions. *Proceedings of JuliaCon*, *1*(1), 1–6. https://doi.org/10.21105/jcon.00058

Araujo Calçada, E., Closset-Kopp, D., Gallet-Moron, E., Lenoir, J., Rêve, M., Hermy, M., & Decocq, G. (2013). Streams are efficient corridors for plant species in forest metacommunities. *Journal of Applied Ecology*, *50*(5), 1152–1160. https://doi.org/10.1111/1365-2664.12132

Baeten, L., Hermy, M., Van Daele, S., & Verheyen, K. (2010). Unexpected understorey community development after 30 years in ancient and post-agricultural forests. *Journal of Ecology*, *98*(6), 1447–1453. https://doi.org/10.1111/j.1365-2745.2010.01711.x

Baeten, L., Sercu, B., Bonte, D., Vanhellemont, M., & Verheyen, K. (2015). Intraspecific variation in flowering phenology affects seed germinability in the forest herb Primula elatior. *Plant Ecology and Evolution*, *148*(2), 283–288. https://doi.org/10.5091/plecevo.2015.1089

Barbet-Massin, M., Jiguet, F., Albert, C. H., & Thuiller, W. (2012). Selecting pseudo-absences for species distribution models: How, where and how many? *Methods in Ecology and Evolution*, *3*(2), 327–338. https://doi.org/10.1111/j.2041-210X.2011.00172.x

Bateman, B. L., Murphy, H. T., Reside, A. E., Mokany, K., & Vanderwal, J. (2013). Appropriateness of full-, partial- and no-dispersal scenarios in climate change impact modelling. *Diversity and Distributions*, *19*(10), 1224–1234. https://doi.org/10.1111/ddi.12107

Benito Garzón, M., Robson, T. M., & Hampe, A. (2019). ΔTraitSDMs: Species distribution models that account for local adaptation and phenotypic plasticity. *New Phytologist*, *222*(4), 1757–1765. https://doi.org/10.1111/nph.15716

Benjamini, Y., & Hochberg, Y. (1995). Controlling the False Discovery Rate: A Practical and Powerful Approach to Multiple Testing. *Journal of the Royal Statistical Society: Series B (Methodological)*, *57*(1), 289–300. http://dx.doi.org/10.1111/j.2517-6161.1995.tb02031.x

Bernhardt-Römermann, M., Baeten, L., Craven, D., De Frenne, P., Hédl, R., Lenoir, J., Bert, D., Brunet, J., Chudomelová, M., Decocq, G., Dierschke, H., Dirnböck, T., Dörfler, I., Heinken, T., Hermy, M., Hommel, P., Jaroszewicz, B., Keczyński, A., Kelly, D. L., … Verheyen, K. (2015). Drivers of temporal changes in temperate forest plant diversity vary across spatial scales. *Global Change Biology*, *21*(10), 3726–3737. https://doi.org/10.1111/gcb.12993

Brus, D. J., Hengeveld, G. M., Walvoort, D. J. J., Goedhart, P. W., Heidema, A. H., Nabuurs, G. J., & Gunia, K. (2012). Statistical mapping of tree species over Europe. *European Journal of Forest Research*, *131*(1), 145–157. http://dx.doi.org/10.1007/s10342-011-0513-5

Buras, A., & Menzel, A. (2019). Projecting tree species composition changes of european forests for 2061–2090 under RCP 4.5 and RCP 8.5 scenarios. *Frontiers in Plant Science*, *9*, 1–13. https://doi.org/10.3389/fpls.2018.01986

Canadell, J. G., & Raupach, M. R. (2008). Managing forests for climate change mitigation. *Science*, *320*(5882), 1456–1457. https://doi.org/10.1126/science.1155458

Chave, J. (2013). The problem of pattern and scale in ecology: What have we learned in 20 years? *Ecology Letters*, *16*(Suppl 1), 4–16. https://doi.org/10.1111/ele.12048

Chytrý, M., Hennekens, S. M., Jiménez-Alfaro, B., Knollová, I., Dengler, J., Jansen, F., Landucci, F., Schaminée, J. H. J., Aćić, S., Agrillo, E., Ambarlı, D., Angelini, P., Apostolova, I., Attorre, F., Berg, C., Bergmeier, E., Biurrun, I., Botta-Dukát, Z., Brisse, H., … Yamalov, S. (2016). European Vegetation Archive (EVA): an integrated database of European vegetation plots. *Applied Vegetation Science*, *19*(1), 173–180. http://dx.doi.org/10.1111/avsc.12191

Clarke, R. T., Rothery, P., & Raybould, A. F. (2002). Confidence limits for regression relationships between distance matrices: Estimating gene flow with distance. *Journal of Agricultural, Biological, and Environmental Statistics*, *7*(3), 361–372. https://doi.org/10.1198/108571102320

Clerici, N., Weissteiner, C. J., Paracchini, M. L., Boschetti, L., Baraldi, A., & Strobl, P. (2013). Pan-European distribution modelling of stream riparian zones based on multi-source Earth Observation data. *Ecological Indicators*, *24*(2013), 211–223. https://doi.org/10.1016/j.ecolind.2012.06.002

Connor, T., Hull, V., Viña, A., Shortridge, A., Tang, Y., Zhang, J., Wang, F., & Liu, J. (2018). Effects of grain size and niche breadth on species distribution modeling. *Ecography*, *41*(8), 1270–1282. https://doi.org/10.1111/ecog.03416

Cook, B. I., Mankin, J. S., Marvel, K., Williams, A. P., Smerdon, J. E., & Anchukaitis, K. J. (2020). Twenty-first century drought projections in the CMIP6 forcing scenarios. *Earth's Future*, *8*(6), 1–20. https://doi.org/10.1029/2019ef001461

Copernicus Land Monitoring Service, European Environment Agency, & European Union. (2020). Pan-European products. *Copernicus*. Copenhagen, Denmark: European Environment Agency. https://land.copernicus.eu/

Cushman, S. A., McKelvey, K. S., Hayden, J., & Schwartz, M. K. (2006). Gene Flow in Complex Landscapes: Testing Multiple Hypotheses with Causal Modeling. *The American Naturalist*, *168*(4), 486–499. http://dx.doi.org/10.1086/506976

Dickson, B. G., Albano, C. M., Anantharaman, R., Beier, P., Fargione, J., Graves, T. A., Gray, M. E., Hall, K. R., Lawler, J. J., Leonard, P. B., Littlefield, C. E., McClure, M. L., Novembre, J., Schloss, C. A., Schumaker, N. H., Shah, V. B., & Theobald, D. M. (2019). Circuit-theory applications to connectivity science and conservation. *Conservation Biology*, *33*(2), 239–249. https://doi.org/10.1111/cobi.13230

Dullinger, S., Dendoncker, N., Gattringer, A., Leitner, M., Mang, T., Moser, D., Mücher, C. A., Plutzar, C., Rounsevell, M., Willner, W., Zimmermann, N. E., & Hülber, K. (2015). Modelling the effect of habitat fragmentation on climate-driven migration of European forest understorey plants. *Diversity and Distributions*, *21*(12), 1375–1387. http://dx.doi.org/10.1111/ddi.12370

Duque-Lazo, J., Navarro-Cerrillo, R. M., & Ruíz-Gómez, F. J. (2018). Assessment of the future stability of cork oak (*Quercus suber* L.) afforestation under climate change scenarios in Southwest Spain. *Forest Ecology and Management*, *409*, 444–456. https://doi.org/10.1016/j.foreco.2017.11.042

Ehrlen, J., & Eriksson, O. (2000). Dispersal Limitation and Patch Occupancy in Forest Herbs. *Ecology*, *81*(6), 1667–1674. http://dx.doi.org/10.2307/177315

Endels, P., Adriaens, D., Verheyen, K., & Hermy, M. (2004). Population structure and adult plant performance of forest herbs in three contrasting habitats. *Ecography*, *27*(2), 225–241. https://doi.org/10.1111/j.0906-7590.2004.03731.x

Engler, R., Hordijk, W., & Guisan, A. (2012). The MIGCLIM R package - seamless integration of dispersal constraints into projections of species distribution models. *Ecography*, *35*(10), 872–878. https://doi.org/10.1111/j.1600-0587.2012.07608.x

European Commission. (2011). State of Europe's forests 2011. https://doi.org/10.1007/s13398-014-0173-7.2

European Commission. (2013). A new EU Forest Strategy: for forests and the forest-based sector. *Communication from the Commission to the Council, the European Parliament, the European Economic and Social Committee and the Committee of the Regions*, *SWD(2013) 342*, 17. https://doi.org/10.1017/CBO9781107415324.004

European Commission. (2019). *Main land-use patterns in the EU within 2015-2030*, JRC Policy Insights, JRC115895. Ispra, Italy: European Commission. https://ec.europa.eu/jrc/en/publication/eur-scientific-and-technical-research-reports/main-land-use-patterns-eu-within-2015-2030

European Commission. (2020). EU Biodiversity Strategy for 2030: Bringing nature back into our lives. *Vol. COM*, *380*. https://doi.org/10.1017/CBO9781107415324.004

European Environment Agency. (2020). *Global and European temperature*. Assessment report from https://www.eea.europa.eu/data-and-maps/indicators/global-and-european-temperature-10/assessment

Fick, S. E., & Hijmans, R. J. (2017). WorldClim 2: New 1-km spatial resolution climate surfaces for global land areas. *International Journal of Climatology*, *37*(12), 4302–4315. https://doi.org/10.1002/joc.5086

Fithian, W., Elith, J., Hastie, T., & Keith, D. A. (2015). Bias correction in species distribution models: Pooling survey and collection data for multiple species. *Methods in Ecology and Evolution*, *6*(4), 424–438. https://doi.org/10.1111/2041-210X.12242

Flanders Research Foundation (FWO). (2020). *Flemish supercomputer center*. https://www.vscentrum.be

Fordham, D. A., Resit Akçakaya, H., Araújo, M. B., Elith, J., Keith, D. A., Pearson, R., & Brook, B. W. (2012). Plant extinction risk under climate change: Are forecast range shifts alone a good indicator of species vulnerability to global warming? *Global Change Biology*, *18*(4), 1357–1371. https://doi.org/10.1111/j.1365-2486.2011.02614.x

Franklin, J. (2010). Moving beyond static species distribution models in support of conservation biogeography. *Diversity and Distributions*, *16*(3), 321–330. https://doi.org/10.1111/j.1472-4642.2010.00641.x

Gederaas, L., Moen, T. L., Skjelseth, S., & Larsen, L.-K. (2012). *Alien species in Norway – with the Norwegian Black List 2012*. Norway: The Norwegian Biodiversity Information Centre. https://www.artsdatabanken.no/Files/13960/Alien_Species_in_Norway_-_with_the_Norwegian_Black_List_2012

Greiser, C., Hylander, K., Meineri, E., Luoto, M., & Ehrlén, J. (2020). Climate limitation at the cold edge: Contrasting perspectives from species distribution modelling and a transplant experiment. *Ecography*, *43*(5), 637–647. https://doi.org/10.1111/ecog.04490

Guisan, A., & Thuiller, W. (2005). Predicting species distribution: Offering more than simple habitat models. *Ecology Letters*, *8*(9), 993–1009. https://doi.org/10.1111/j.1461-0248.2005.00792.x

Guisan, A., & Zimmermann, N. E. (2000). Predictive habitat distribution models in ecology. *Ecological Modelling*, *135*(2-3), 147–186. http://dx.doi.org/10.1016/s0304-3800(00)00354-9

Guisan, A., Zimmermann, N. E., & Thuiller, W. (2017). Habitat suitability and distribution models. *Ecology, Biodiversity and Conservation*, Cambridge: Cambridge University Press. https://doi.org/10.1017/9781139028271

Guo, F., Lenoir, J., & Bonebrake, T. C. (2018). Land-use change interacts with climate to determine elevational species redistribution. *Nature Communications*, *9*(1315), 1–7. https://doi.org/10.1038/s41467-018-03786-9

Gustafson, E. J., & Parker, G. R. (1994). Using an index of habitat patch proximity for landscape design. *Landscape and Urban Planning*, *29*(2-3), 117–130. https://doi.org/10.1016/0169-2046(94)90022-1

Hennekens, S. M., Smits, N. A. C., & Schaminée, J. H. J. (2010). *SynBioSys 3.3.1*. Alterra, Wageningen UR. https://www.synbiosys.alterra.nl/synbiosysnl/

Hesselbarth, M. H. K., Sciaini, M., With, K. A., Wiegand, K., & Nowosad, J. (2019). Landscapemetrics: An open-source R tool to calculate landscape metrics. *Ecography*, *42*(10), 1648–1657, https://doi.org/10.1111/ecog.04617

Hiederer, R. (2013). Mapping soil properties for Europe - spatial representation of soil database attributes. *JRC Technical Reports*. https://doi.org/10.2788/94128

Hijmans, R. J. (2019). *raster: Geographic data analysis and modeling. R package version 3.0-7*. https://cran.r-project.org/web/packages/raster/raster.pdf

Hijmans, R. J., Phillips, S., Leathwick, J., & Elith, J. (2017). *dismo: Species distribution modeling version 1.1-4*. https://cran.r-project.org/package=dismo

Honnay, O., Butaye, J., Jacquemyn, H., Verheyen, K., Hermy, M., Bossuyt, B., & Bossuyt, B. (2002). Possible effects of habitat fragmentation and climate change on the range of forest plant species. *Ecology Letters*, *5*(4), 525–530. https://doi.org/10.1046/j.1461-0248.2002.00346.x

Hunter-Ayad, J., Ohlemüller, R., Recio, M. R., & Seddon, P. J. (2020). Reintroduction modelling: A guide to choosing and combining models for species reintroductions. *Journal of Applied Ecology*, *57*(7), 1233–1243. http://dx.doi.org/10.1111/1365-2664.13629

Jacquemyn, H., Brys, R., & Hermy, M. (2002). Patch occupancy, population size and reproductive success of a forest herb (Primula elatior) in a fragmented landscape. *Oecologia*, *130*(4), 617–625. https://doi.org/10.1007/s00442-001-0833-0

Jacquemyn, H., Vandepitte, K., Roldán-Ruiz, I., & Honnay, O. (2009). Rapid loss of genetic variation in a founding population of primula elatior (primulaceae) after colonization. *Annals of Botany*, *103*(5), 777–783. https://doi.org/10.1093/aob/mcn253

Koen, E. L., Bowman, J., & Walpole, A. A. (2012). The effect of cost surface parameterization on landscape resistance estimates. *Molecular Ecology Resources*, *12*(4), 686–696. https://doi.org/10.1111/j.1755-0998.2012.03123.x

Konečná, V., Nowak, M. D., & Kolář, F. (2019). Parallel colonization of subalpine habitats in the central European mountains by primula elatior. *Scientific Reports*, *9*(1), 0–12. https://doi.org/10.1038/s41598-019-39669-2

Krosby, M., Tewksbury, J., Haddad, N. M., & Hoekstra, J. (2010). Ecological connectivity for a changing climate. *Conservation Biology*, *24*(6), 1686–1689. https://doi.org/10.1111/j.1523-1739.2010.01585.x

Laliberté, J., & St-Laurent, M. H. (2020). Validation of functional connectivity modeling: The achilles' heel of landscape connectivity mapping. *Landscape and Urban Planning*, *202*, 103878. https://doi.org/10.1016/j.landurbplan.2020.103878

Landguth, E. L., Building, M., Collins, F., Agra, C., & Vaira, D. (2010). Relationships between migration rates and landscape resistance assessed using individual-based simulations. *Molecular Ecology*, *10*, 854–862. https://doi.org/10.1111/j.1755-0998.2010.02867.x

Landuyt, D., De Lombaerde, E., Perring, M. P., Hertzog, L. R., Ampoorter, E., Maes, S. L., & Verheyen, K. (2019). The functional role of temperate forest understorey vegetation in a changing world. *Global Change Biology*, *25*(11), 3625–3641. https://doi.org/10.1111/gcb.14756

Lassueur, T., Joost, S., & Randin, C. F. (2006). Very high resolution digital elevation models: Do they improve models of plant species distribution? *Ecological Modelling*, *198*(1–2), 139–153. https://doi.org/10.1016/j.ecolmodel.2006.04.004

Lavalle, C. (2014). *Land-use/cover maps (LUISA Platform REF2014)*. European Commission, Joint Research Centre. http://data.europa.eu/89h/jrc-luisa-land-use-ref-2014

Lembrechts, J. J., Nijs, I., & Lenoir, J. (2018). Incorporating microclimate into species distribution models. *Ecography*, 1267–1279. https://doi.org/10.1111/ecog.03947

Lenoir, J., & Svenning, J. C. (2015). Climate-related range shifts - a global multidimensional synthesis and new research directions. *Ecography*, *38*(1), 15–28. https://doi.org/10.1111/ecog.00967

Leuschner, C., & Ellenberg, H. (2017). *Ecology of central European forests: Vegetation ecology of central Europe* (Vol. *1*). Springer.

Littlefield, C. E., McRae, B. H., Michalak, J. L., Lawler, J. J., & Carroll, C. (2017). Connecting today's climates to future climate analogs to facilitate movement of species under climate change. *Conservation Biology*, *31*(6), 1397–1408. https://doi.org/10.1111/cobi.12938

Liu, C., White, M., & Newell, G. (2013). Selecting thresholds for the prediction of species occurrence with presence-only data. *Journal of Biogeography*, *40*(4), 778–789. https://doi.org/10.1111/jbi.12058

Lunt, I. D., Byrne, M., Hellmann, J. J., Mitchell, N. J., Garnett, S. T., Hayward, M. W., Martin, T. G., Mcdonald-maddden, E., Williams, S. E., & Zander, K. K. (2013). Using assisted colonisation to conserve

biodiversity and restore ecosystem function under climate change. *Biological Conservation*, *157*, 172–177. https://doi.org/10.1016/j.biocon.2012.08.034

Maiorano, L., Chiaverini, L., Falco, M., & Ciucci, P. (2019). Combining multi-state species distribution models, mortality estimates, and landscape connectivity to model potential species distribution for endangered species in human dominated landscapes. *Biological Conservation*, *237*, 19–27. https://doi.org/10.1016/j.biocon.2019.06.014

McDowell, N. G., Williams, A. P., Xu, C., Pockman, W. T., Dickman, L. T., Sevanto, S., & Koven, C. (2016). Multi-scale predictions of massive conifer mortality due to chronic temperature rise. *Nature Climate Change*, *6*(3), 295–300. https://doi.org/10.1038/nclimate2873

McRae, B. H. (2006). Isolation by resistance. *Evolution*, *60*(8), 1551–1561. http://dx.doi.org/10.1554/05-321.1

McRae, B. H., Dickson, B. G., Keitt, T. H., & Shah, V. B. (2008). Using circuit theory to model connectivity in ecology, evolution, and conservation. *Ecology*, *89*(10), 2712–2724. https://doi.org/10.1890/07-1861.1

McRae, B. H., & Shah, V. B. (2011). CIRCUITSCAPE User Guide. *The University of California, Santa Barbara, January 2009*. http://www.circuitscape.org

Merow, C., Smith, M. J., & Silander, J. A. (2013). A practical guide to MaxEnt for modeling species' distributions: What it does, and why inputs and settings matter. *Ecography*, *36*(10), 1058–1069. https://doi.org/10.1111/j.1600-0587.2013.07872.x

Millar, C. I., Stephenson, N. L., & Stephens, S. L. (2007). Climate change and forests of the future: Managing in the face of uncertainty. *Ecological Applications*, *17*(8), 2145–2151. https://doi.org/10.1890/06-1715.1

Moore, R. D., Spittlehouse, D. L., & Story, A. (2005). Riparian microclimate and stream temperature response to forest harvesting: A review. *Journal of the American Water Resources Association*, *41*(4), 813–834. https://doi.org/10.1111/j.1752-1688.2005.tb04465.x

Muscarella, R., Galante, P. J., Soley-Guardia, M., Boria, R. A., Kass, J., Uriarte, M., & Anderson, R. P. (2014). ENMeval: An R package for conducting spatially independent evaluations and estimating optimal model complexity for ecological niche models. *Methods in Ecology and Evolution*, *11*(5), 1198–1205.

Naaf, T., & Kolk, J. (2015). Colonization credit of post-agricultural forest patches in NE Germany remains 130–230 years after reforestation. *Biological Conservation*, *182*, 155–163. https://doi.org/10.1016/j.biocon.2014.12.002

Nei, M. (1978). Estimation of average heterozygosity and genetic distance from a small number of individuals. *Genetics*, *89*(3), 583–590. https://doi.org/10.1093/genetics/89.3.583

Nenzén, H. K., & Araújo, M. B. (2011). Choice of threshold alters projections of species range shifts under climate change. *Ecological Modelling*, *222*(18), 3346–3354. https://doi.org/10.1016/j.ecolmodel.2011.07.011

Nieto-Lugilde, D., Lenoir, J., Abdulhak, S., Aeschimann, D., Dullinger, S., Gégout, J. C., & Svenning, J. C. (2015). Tree cover at fine and coarse spatial grains interacts with shade tolerance to shape plant species distributions across the Alps. *Ecography*, *38*(6), 578–589. https://doi.org/10.1111/ecog.00954

Peterman, W. E. (2018). ResistanceGA: An R package for the optimization of resistance surfaces using genetic algorithms. *Methods in Ecology and Evolution*, *9*(6), 1638–1647. http://dx.doi.org/10.1111/2041-210x.12984

Peterman, W. E., Winiarski, K. J., Moore, C. E., Carvalho, C. D. S., Gilbert, A. L., & Spear, S. F. (2019). A comparison of popular approaches to optimize landscape resistance surfaces. *Landscape Ecology*, *34*, 2197–2208. https://doi.org/10.1007/s10980-019-00870-3

Phillips, S. J., Anderson, R. P., Dudík, M., Schapire, R. E., & Blair, M. E. (2017). Opening the black box: An open-source release of Maxent. *Ecography*, *40*(7), 887–893. https://doi.org/10.1111/ecog.03049

Phillips, S. J., & Dudík, M. (2008). Modeling of species distributions with Maxent: new extensions and a comprehensive evaluation. *Ecography*, *31*(2), 161–175. http://dx.doi.org/10.1111/j.0906-7590.2008.5203.x.

Phillips, S. J., Dudík, M., & Schapire, R. E. (2020). Maxent software for modeling species niches and distributions (Version 3.4.3). Available at: http://biodiversityinformatics.amnh.org/open_source/maxent/. Accessed November 20, 2020.

Razgour, O., Forester, B., Taggart, J. B., Bekaert, M., Juste, J., Ibáñez, C., & Manel, S. (2019). Considering adaptive genetic variation in climate change vulnerability assessment reduces species range loss projections. *Proceedings of the National Academy of Sciences of the United States of America*, *116*(21), 10418–10423. https://doi.org/10.1073/pnas.1820663116

Sirami, C., Caplat, P., Popy, S., Clamens, A., Arlettaz, R., Jiguet, F., Brotons, L., & Martin, J. L. (2017). Impacts of global change on species distributions: Obstacles and solutions to integrate climate and land use. *Global Ecology and Biogeography*, *26*(4), 385–394. https://doi.org/10.1111/geb.12555

Skov, F., & Svenning, J. C. (2004). Potential impact of climatic change on the distribution of forest herbs in Europe. *Ecography*, *27*(3), 366–380. https://doi.org/10.1111/j.0906-7590.2004.03823.x

Spiecker, H., Hansen, J., Klimo, E., Skovsgaard, J. P., Sterba, H., & von Teuffel, K. (2004). Norway Spruce Conversion – Options and Consequences. EFI Research Report 18. Brill: Leiden, Boston, Köln.

Takahashi, K., & Kamitani, T. (2004). Effect of dispersal capacity on forest plant migration at a landscape scale. *Journal of Ecology*, *92*(5), 778–785. http://dx.doi.org/10.1111/j.0022-0477.2004.00927.x

Taylor, K., & Woodell, S. R. J. (2008). Biological flora of the British isles: Primula elatior (L.) Hill. *Journal of Ecology*, *96*(5), 1098–1116. https://doi.org/10.1111/j.1365-2745.2008.01418.x

Thuiller, W., Lavorel, S., Araújo, M. B., Sykes, M. T., & Prentice, I. C. (2005). Climate change threats to plant diversity in Europe. *Proceedings of the National Academy of Sciences of the United States of America*, *102*(23), 8245–8250. https://doi.org/10.1073/pnas.0409902102

Thuiller, W., Pollock, L. J., Gueguen, M., & Münkemüller, T. (2015). From species distributions to meta-communities. *Ecology Letters*, *18*(12), 1321–1328. https://doi.org/10.1111/ele.12526

Valdés, A., Lenoir, J., Gallet-Moron, E., Andrieu, E., Brunet, J., Chabrerie, O., … Decocq, G. (2015). The contribution of patch-scale conditions is greater than that of macroclimate in explaining local plant diversity in fragmented forests across Europe. *Global Ecology and Biogeography*, *24*(9), 1094–1105. https://doi.org/10.1111/geb.12345

Van Strien, M. J., Holderegger, R., & Van Heck, H. J. (2015). Isolation-by-distance in landscapes: Considerations for landscape genetics. *Heredity*, *114*(1), 27–37. https://doi.org/10.1038/hdy.2014.62

Veloz, S. D. (2009). Spatially autocorrelated sampling falsely inflates measures of accuracy for presence-only niche models. *Journal of Biogeography*, *36*(12), 2290–2299. https://doi.org/10.1111/j.1365-2699.2009.02174.x

Verheyen, K., Honnay, O., Motzkin, G., Hermy, M., & Foster, D. R. (2003). Response of forest plant species to land-use change: A life-history trait-based approach. *Journal of Ecology*, *91*(4), 563–577. https://doi.org/10.1046/j.1365-2745.2003.00789.x

Vittoz, P., & Engler, R. (2007). Seed dispersal distances: A typology based on dispersal modes and plant traits. *Botanica Helvetica*, *117*, 109–124. https://doi.org/10.1007/s00035-007-0797-8

Warren, D. L., & Seifert, S. N. (2011). Ecological niche modeling in Maxent: the importance of model complexity and the performance of model selection criteria. *Ecological Applications*, *21*(2), 335–342. http://dx.doi.org/10.1890/10-1171.1

Wessinger, C. A., Kelly, J. K., Jiang, P., Rausher, M. D., & Hileman, L. C. (2018). SNP-skimming: A fast approach to map loci generating quantitative variation in natural populations. *Molecular Ecology Resources*, *18*(6), 1402–1414. https://doi.org/10.1111/1755-0998.12930

Whale, D. M. (1983). The response of primula species to soil waterlogging and soil drought. *International Association for Ecology*, *58*(2), 272–277. https://doi.org/10.1007/BF00399231

Zellweger, F., De Frenne, P., Lenoir, J., Vangansbeke, P., Verheyen, K., Bernhardt-Römermann, M., … Coomes, D. (2020). Forest microclimate dynamics drive plant responses to warming. *Science*, *368*(6492), 772–775.

BIOSKETCH

Frederik Van Daele is a research fellow examining how plant species translocations can be informed by modelling and genomic data. His main research interest is the importance of ecological patterns in landscape restoration and planning.

Olivier Honnay is a Professor of Plant Conservation Biology and focusses on the effects of anthropogenic disturbances on plant species richness and genetic diversity.

Hanne De Kort is a post-doctoral research fellow interested in exploring patterns of molecular diversity across species' ranges and in understanding population dynamics and environmental factors driving these patterns.

SUPPORTING INFORMATION

Additional supporting information may be found online in the Supporting Information section.

How to cite this article: Van Daele, F., Honnay, O., & De Kort, H. (2021). The role of dispersal limitation and reforestation in shaping the distributional shift of a forest herb under climate change. *Diversity and Distributions*, 27, 1775–1791. https://doi.org/10.1111/ddi.13367